

## RESEARCH ARTICLE

# A theoretical perspective of the ultrafast transient absorption dynamics of CsPbBr<sub>3</sub>

Ariadni Boziki | Pablo Baudin | Elisa Liberatore | Negar Ashari Astani | Ursula Rothlisberger

Laboratory of Computational Chemistry and Biochemistry, Institute of Chemical Sciences and Engineering, École Polytechnique Fédérale de Lausanne, Lausanne, Switzerland

## Correspondence

Ursula Rothlisberger, Laboratory of Computational Chemistry and Biochemistry, Institute of Chemical Sciences and Engineering, École Polytechnique Fédérale de Lausanne, CH-1015 Lausanne, Switzerland.  
Email: ursula.rothlisberger@epfl.ch

## Present address

Negar Ashari Astani, Department of Physics and Energy Engineering, Amirkabir University of Technology, Tehran, Iran

## Funding information

Schweizerischer Nationalfonds zur Förderung der Wissenschaftlichen Forschung, Grant/Award Number: 200020-185092

## Abstract

Transient absorption spectra (TAS) of lead halide perovskites can provide important insights into the nature of the photoexcited state dynamics of this prototypical class of materials. Here, we perform ground and excited state molecular dynamics (MD) simulations within a restricted open shell Kohn-Sham (ROKS) approach in order to interpret the characteristic features of the TAS of CsPbBr<sub>3</sub>. Our results reveal that properties such as the finite temperature band gap, the Stokes shift, and therefore, also the TAS are strongly size-dependent. Our TAS simulations show an early positive red-shifted feature on the fs scale that can be explained by geometric relaxation in the excited state. As excited-state processes can crucially affect the electronic properties of this class of photoactive materials, our observations are an important ingredient for further optimization of lead halide based optoelectronic devices.

## KEYWORDS

absorption spectra, CsPbBr<sub>3</sub>, excited state dynamics, molecular dynamics, ROKS, Stokes shifts, transient absorption spectra

## 1 | INTRODUCTION

Over the last years, organic–inorganic lead halide perovskites have attracted great attention because of their impressive photovoltaic performance and their superb photoluminescence properties, which also render them a suitable choice for making perovskite light-emitting diodes (LEDs).<sup>1–10</sup> Despite the rapid progress in device fabrication, a thorough understanding of the fundamental nature of the excited states of this class of materials is still missing.<sup>11–17</sup> Such characterization is an important ingredient for further optimization, as excited-state processes can crucially affect the optoelectronic performance.

Among the different lead halide perovskites,<sup>2–5,7</sup> CsPbBr<sub>3</sub> is especially suited for investigations of the excited state dynamics via transient absorption spectroscopy experiments due to its higher photostability compared to other organic–inorganic lead halide perovskites.<sup>11,18–26</sup> The

large band gap of CsPbBr<sub>3</sub> that lies within the range of 2.25–2.36 eV according to measurements performed by different groups,<sup>22,27</sup> prevents direct photovoltaic application, but CsPbBr<sub>3</sub> is instead a promising material for LEDs and laser applications.<sup>9,10,28,29</sup>

Although several femtosecond transient absorption spectroscopy measurements have been conducted for MAPbI<sub>3</sub>, MAPbBr<sub>3</sub>, and CsPbBr<sub>3</sub>,<sup>14,15,17,23,24,30–32</sup> the interpretation of the mechanistic origin of the observed features is still under debate. More specifically, ultrafast transient absorption studies of cubic CsPbBr<sub>3</sub> nanocrystals as a function of size showed that for small nanocrystals of ~4 nm edge length, strong quantum confinement effects are manifested in the excited-state dynamics that differ from the ones observed for the bulk material.<sup>33</sup> In addition to the size-dependent TAS, size-dependent absorption spectra and size-dependent Stokes shifts were revealed when photoluminescence measurements of CsPbBr<sub>3</sub> nanocrystals were

This is an open access article under the terms of the Creative Commons Attribution-NonCommercial-NoDerivs License, which permits use and distribution in any medium, provided the original work is properly cited, the use is non-commercial and no modifications or adaptations are made.

© 2022 The Authors. *Journal of Computational Chemistry* published by Wiley Periodicals LLC.

performed.<sup>11,33,34</sup> In order to understand the origin of the Stokes shift in CsPbBr<sub>3</sub> nanocrystals, Brennan et al.,<sup>35</sup> performed static density functional theory (DFT) calculations of the band structure, suggesting that for particles between 2 and 5 nm size, the observed shift is due to the existence of an intrinsic confined hole state 70–260 meV above the valence band edge which is relatively dark in absorption due to its low density of states, but bright in emission.

The time-dependent transient absorption measurements of CsPbBr<sub>3</sub> performed by Yarita et al.<sup>17</sup> revealed an early (0.4 ps) evolution of a positive transient absorption signal at 509 nm and a negative one at 528 nm. The latter signal disappeared at later time delays ( $\geq 7.5$  ps) giving rise to a unique positive feature. Ultrafast transient absorption spectroscopy that was used to investigate the origin of the exceptionally high photoluminescence quantum yield of CsPbBr<sub>3</sub> quantum dots,<sup>23</sup> showed an exciton bleaching feature at  $\sim 480$  nm at early time delays (0.2–0.5 ps) and an exciton absorption feature at  $\sim 495$  nm at the same delay, which the authors assigned to state-filling-induced bleach and hot-exciton-induced red-shift, respectively. After the hot-exciton relaxation ( $\geq 2$  ps), the exciton-induced shift disappeared and the TAS was solely dominated by the exciton bleaching feature.<sup>23</sup> According to the authors, the high photoluminescence quantum yield of CsPbBr<sub>3</sub> quantum dots is a result of the negligible electron- and hole-trapping pathways.

On the other hand, Wei et al.<sup>24</sup> observed three features in the 0.1 ps time delay time-dependent TAS of CsPbBr<sub>3</sub> quantum dots with average edge length of 11.4 nm. A band of photoinduced bleach at 510 nm and two bands of photoinduced absorptions; the first one being very well-resolved and centered at 521 nm, while the second was subtle, with a small amplitude and very wide spectrum throughout the visible region.<sup>24</sup> At later time delays, after 2–5 ps, although there were still some contributions from the two bands of photoinduced absorptions, the TAS was dominated by the band of photoinduced bleach. The authors attributed the 0.1 ps time delay TAS mostly to a carrier-induced Stark effect, and they also correlated the red-shift of the energies with two-body recombination possibly due to a strong coupling between excitons.<sup>24</sup>

The debate between the various interpretations regarding the features of the TAS of CsPbBr<sub>3</sub>, calls for further studies to shed light on the mechanistic origin, and on fundamental issues related to the excited state of organic–inorganic lead halide perovskites in general. In this work, we perform transient absorption simulations of CsPbBr<sub>3</sub> at early time delays using Car-Parrinello MD coupled with ROKS. For the simulations we use two different cell sizes, probing the size-dependent nature of the finite temperature band gap, the Stokes shift and the TAS. To the best of our knowledge, so far all theoretical interpretations of the TAS were based on static calculations, while here we employ a dynamic approach for simulating the TAS of CsPbBr<sub>3</sub>.

## 2 | RESULTS AND DISCUSSION

For the simulation of TAS, we considered an approach similar to the one followed in transient absorption experiments. More specifically,

transient absorption spectroscopy is a time-resolved technique that allows monitoring the absorption spectrum of a sample after photoexcitation through a probe laser pulse at different delay times with respect to the pump pulse. In detail, when a sample is photoexcited, its absorption spectrum is modified due to the different distribution of the photoinduced charge carriers.<sup>36</sup> The transient absorption signal  $\Delta A$  at a certain delay time  $\tau$  is defined as the difference between the pumped  $A(E, \tau)$  and unpumped  $A(E)$  signals, as described by Equation 1.<sup>36</sup>

$$\Delta A(E, \tau) = A(E, \tau) - A(E, \tau = 0). \quad (1)$$

The result of a transient absorption spectroscopy measurement is thus a differential absorption signal that is a function of both probe photon energy and time delay.

As a first test of the computational scheme, we checked if we can reproduce the experimentally observed Stokes shift of CsPbBr<sub>3</sub>.<sup>11,33,34</sup> For this purpose, we exploited the more expedient ROKS approach, a DFT-based method that describes the first non-degenerate excited singlet state of a system.<sup>37</sup> The absorption and emission energies at 0 K were calculated using the real-space equivalent of the fully k-point sampled system of the most stable phase of CsPbBr<sub>3</sub> at room temperature,<sup>38</sup> the orthorhombic phase. The experimental structure of CsPbBr<sub>3</sub> is shown in Figure 1. Benchmark calculations showed that such an appropriate real-space analog can be found with a supercell containing 160 atoms. The 0 K band gap of this system is 2.08 eV compared to the fully converged value of 2.13 eV. The energy differences between the ground state and the first excited state for the ground state optimized structure and the first excited state optimized counterpart, that is, the Stokes shift are calculated for

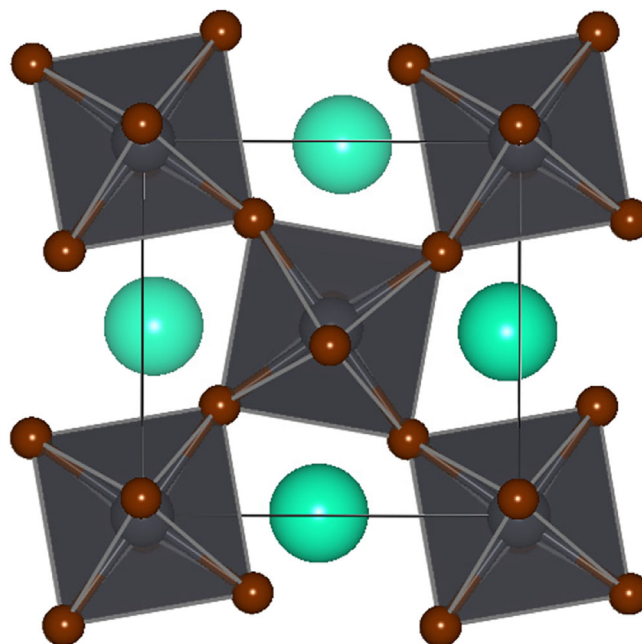


**FIGURE 1** Experimental crystal structure of CsPbBr<sub>3</sub>. Cs<sup>+</sup> (green balls), Br<sup>-</sup> (brown balls), Pb<sup>2+</sup> (silver balls)

the 160 atom system. ROKS predicts a Stokes shift of 0.02 eV fully consistent with experimental results for bulk CsPbBr<sub>3</sub> of roughly 0.02 eV indicating the adequacy of the ROKS method for describing the excited state dynamics in this system.<sup>35</sup>

In order to calculate the TAS, we exploited Equation (1) and computed the difference between the excited state absorption spectra and its ground state counterpart at different time delays. For this, we first calculated the steady state absorption spectrum by performing Car-Parrinello MD simulations of the ground state at 300 K for the super cell containing 160 atoms. For the estimation of the finite temperature band gap, 166 configurations were sampled from the equilibrated trajectory of 9.5 ps and the probability distribution of the Kohn-Sham band gaps are shown in Figure 2.

Since spin-orbit coupling is known to be strong in lead halide perovskites, we also determined the analogous spectrum for triplet state.<sup>39</sup> The triplet state is determined by performing single point calculations for the same configurations that have been used in the calculation of the Kohn-Sham band gaps but using different spin multiplicity. As shown in Figure 2, the probability distributions overlap with each other suggesting that both singlet and triplet states can contribute to the absorption spectrum of CsPbBr<sub>3</sub> in similar ways. Furthermore, the maximum of the peak for both singlet and triplet transitions is 2.11–2.12 eV showing that the band gap experiences a slight (0.04 eV) blue-shift at finite temperatures. This observation is at variance with the behavior of classical semiconductors,<sup>40–42</sup> but is consistent with previous work on lead halide perovskites, where typical blue-shifts of the order of 0.01–0.03 eV have been observed,<sup>43</sup> and can be rationalized in terms of the decrease in antibonding orbital overlap of the divalent cation and anion orbitals that make up the band edges (vide supra) due to thermal fluctuations. To further support the argument that the probability distribution of the Kohn-Sham band gaps of CsPbBr<sub>3</sub> can represent its steady state absorption

spectrum, we calculated the absorption spectrum using TDDFT. In Figure S1, the absorption spectrum of CsPbBr<sub>3</sub>, including only the first excited state is shown. The maximum of the peaks of both spectra (Figure 1 and Figure S1) are the same supporting that the probability distribution of the Kohn-Sham band gaps can be safely used in the simulation of the TAS.

For the simulations of the TAS, because of the high computational cost for excited state simulations and the necessity to perform a sufficient number of independent trajectories, we performed the excited state dynamics with a smaller system containing a single unit cell of the orthorhombic structure with 20 atoms. Furthermore, comparing the electronic properties of this smaller size system with the results obtained for the 160 atom super cell, we could also gain information about possible size effects on the steady-state absorption spectrum and the Stokes shift.<sup>11,33–35</sup> Following the approach described above to calculate the Stokes shift and finite temperature band gap (Figure 3), we find that for this smaller size system the Stokes shift is 0.24 eV, that is, larger than in the case of the simulation box with 160 atoms. A similar increase in the Stokes shift from ~30 to 100 meV with decreasing crystal size (from 11.7 to 4.1 nm), has been reported in experiments of CsPbBr<sub>3</sub> perovskite nanocrystals.<sup>35</sup>

In addition, we find that for this smaller size system temperature effects lead to a more pronounced blue-shift of the steady-state spectrum. In fact, the maximum of the band for the lowest singlet and triplet Kohn-Sham single-particle excitations (Figure 3) lies at 2.75 and 2.68 eV, respectively. This is fully consistent with the blue-shifted absorption spectrum of previously reported experiments of CsPbBr<sub>3</sub> perovskite quantum dots and nanocrystals upon decrease of the system size.<sup>11,33</sup>

As mentioned above, for the calculation of the TAS, we exploited Equation (1) and subtracted the simulated steady-state absorption spectrum from the probability distribution of the first excited-state

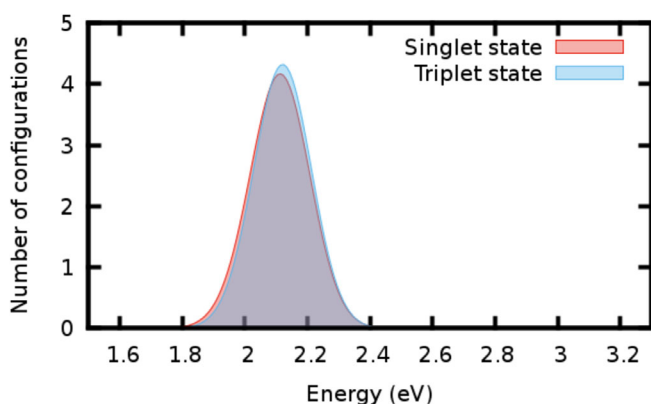


**FIGURE 2** Probability distribution of the Kohn-Sham band gaps (for both singlet and triplet states) of CsPbBr<sub>3</sub>, at 300 K for a simulation box containing 160 atoms. For the estimation of the finite temperature band gap, 166 configurations were sampled from the equilibrated ground-state trajectory. The maximum of the peak for singlet and triplet states is nearly identical (2.11 and 2.12 eV, respectively). The data have been fitted to a Gaussian function for better visibility

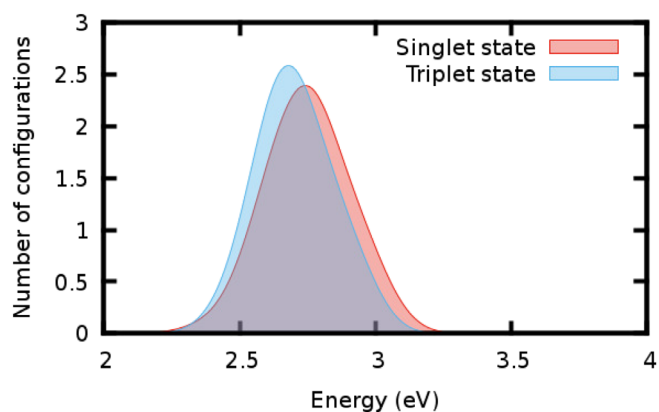


**FIGURE 3** Probability distribution of the Kohn-Sham band gaps (for both singlet and triplet states) of CsPbBr<sub>3</sub> when a simulation box of 20 atoms is employed. For the estimation of the finite temperature band gap, 560 configurations were sampled from the equilibrated ground-state trajectory. The maximum of the peak for singlet and triplet states is 2.75 and 2.68 eV, respectively. The data have been fitted to a Gaussian function for better visibility

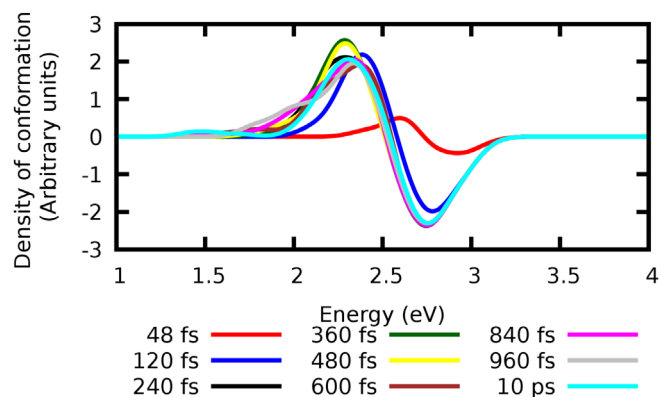


**FIGURE 4** TAS for a simulation box of 20 atoms of CsPbBr<sub>3</sub> at 300 K, simulated with ROKS. The data have been fitted to Gaussian functions for better visibility. All oscillator strengths were assumed to be the same given that they involve transitions into the same state at very similar geometries

excitations at different time delays. For this reason, we performed 100 ROKS excited state dynamics simulations for the system of 20 atoms. In Figure 4, the simulated TAS are shown. After 120 fs the spectra experiences a red-shift indicated by the appearance of a positive peak at 2.42 eV, which can be attributed to the excited state geometric relaxation and whose magnitude is equal to the Stokes shift, accompanied by a negative feature at 2.79 eV due to ground state bleaching. These features have also been previously reported in transient absorption experiments of CsPbBr<sub>3</sub> nanocrystals and quantum dots for short time delays.<sup>17,23,24</sup> For larger time delays, the main qualitative features are similar to the absorption spectrum in the ground state and the excited spectra are basically identical with the contributions to the TAS due to geometric changes being negligible. For an easier analysis of the spectra, we are also plotting them for different time delay ranges (Figure 5). It is worth mentioning that calculations that aimed at interpreting the TAS of MAPbI<sub>3</sub> exploiting the contribution of different conduction and valence band pairs to the optical properties and not taking into account the excited-state geometric relaxation could not reproduce the early positive red-shifted feature.<sup>32</sup> The absence of this feature following this approach further supports our suggestion that the early red-shifted feature is due to excited-state geometric relaxation. To further support our suggestion we examined the geometric distortions by comparing the Pb-Br distances of the ground-state trajectory at 300 K with the ones of the excited-state trajectories. We notice that the ground-state trajectory has only one set of similar Pb-Br distances, which average is 3.05 Å. On the other hand, the Pb-Br distances extracted from the excited-state dynamics trajectory can be classified into two different sets, which averages are 3.23 and 2.99 Å, accordingly.

We also simulated TAS performing two ROKS excited state dynamics simulations using the 160 atoms system. Our simulations (Figure S2 in Supporting Information) showed that the main qualitative features of the spectra are similar to the ones of the cell of 20 atoms but again showing a strong size effect in the band positions confirming the size-dependent nature of TAS. However, we were not able to perform a

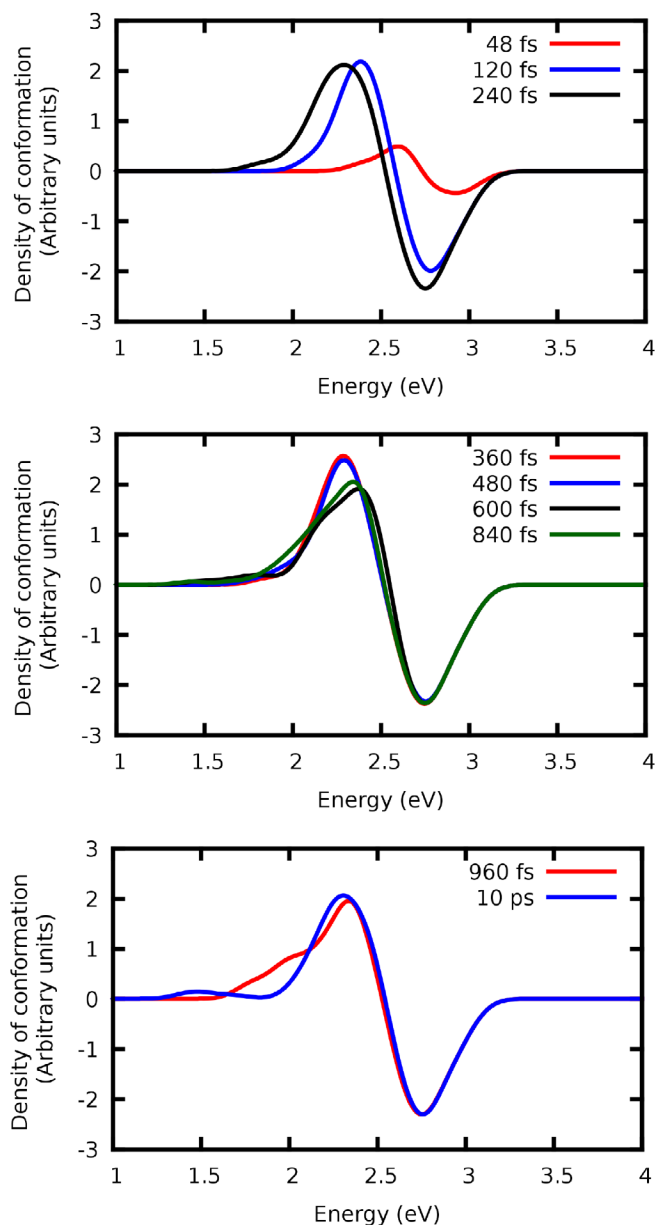


**FIGURE 5** TAS for a simulation box of 20 atoms of CsPbBr<sub>3</sub> at 300 K, simulated with ROKS plotted for different time delay ranges. The data have been fitted to Gaussian functions for better visibility

sufficient number of simulations with the 160 atoms cell to fully converge the spectrum with respect to sampled configurations due to the high computational cost. Furthermore, we performed simulations of the Stokes shift, the steady-state absorption spectrum as well as the TAS employing linear-response time-dependent density functional theory (LR-TDDFT). These calculations also showed strong size-dependent behavior (Figures S3 and S4 in Supporting Information).

### 3 | CONCLUSIONS

Although several transient absorption spectroscopy measurements have been conducted for CsPbBr<sub>3</sub>,<sup>17,23,24</sup> the debate between the

various interpretations regarding the features of the TAS, calls for further studies to shed light on the mechanistic origin related to the excited state of this material. Here, we propose a theoretical protocol to study and interpret the early-time features of the TAS in order to study the TAS of CsPbBr<sub>3</sub> and lead halide perovskites in general.

The computational approach is able to reproduce also the finite temperature band gap and Stokes shift of CsPbBr<sub>3</sub>. We observe that properties such as the finite temperature band gap and the Stokes shift are strongly size-dependent. In analogy to these size-dependent properties, the TAS is also size-dependent. The simulated features of TAS agree well with experimental measurements. More specifically, an early positive red-shifted feature in the fs scale dynamics that can be explained by geometric relaxation in the excited-state has been revealed. For larger time delays, the main qualitative features are similar to the absorption spectrum in the ground state and the excited state spectra are basically identical with the contributions to the TAS due to geometric changes being negligible.

Our approach includes the differences between the excited and ground state geometries as factors that could contribute to the transient absorption measurements exploiting the relaxation of the structure in excited states. Other effects such as band gap renormalization, many-body effects and excitonic effects cannot be captured with this approach. However, the existence of a Stokes shift is the first indication of the importance of geometric relaxations for the excited state dynamics. In any case, there are claims that the impact of some of the effects that our approach cannot capture is not so significant. For example, the small exciton binding energy is a characteristic of three-dimensional halide perovskites.<sup>44–46</sup> To the best of our knowledge, a dynamical approach for the simulation of the TAS of lead halide perovskites has not been employed so far. Our results allow us to understand the mechanistic origin of the excited state of this material, paving the way for further optimization of this special class of materials.

## 4 | COMPUTATIONAL DETAILS

DFT<sup>47,48</sup> static calculations have been performed using the Quantum Espresso suite of codes,<sup>49,50</sup> while the CPMD code was used for dynamics.<sup>51</sup> The generalized gradient approximation to DFT in the PBE formulation has been used.<sup>52</sup> Scalar relativistic effects have been included via the pseudopotentials while explicit spin-orbit couplings have not been taken into account in view of the well-known fortuitous error cancellation between spin orbit coupling and many-body effects described e.g. by means of GW-self energy correction.<sup>39,53,54</sup>

Quantum Espresso was chosen for the band gap calculations at 0 K, with a sampling of the Brillouin zone with a  $7 \times 7 \times 7$  Monkhorst-Pack shifted  $k$ -point grid.<sup>55</sup> To calculate the corresponding gap of the real-space sample, the CPMD code was used instead. In Quantum Espresso calculations, the interactions between valence electrons, core electrons and nuclei are described by ultrasoft pseudopotentials.<sup>56</sup> The Kohn-Sham orbitals are expanded in a plane wave basis set with a kinetic energy cutoff of 40 Ry and a density cutoff of 240 Ry. The above

values have been chosen after having performed convergence tests for the total energy, the band gap, the pressure, the stresses and the atomic forces. For the calculations with CPMD, the wavefunction cut-off was set to 90 Ry and Goedecker normconserving pseudopotentials were employed.<sup>57–59</sup>

Car-Parrinello MD simulations for the ground state in the NVT ensemble were performed using the CPMD code.<sup>51</sup> A time step of 5 a. u. was used with a fictitious mass parameter of 800 a.u. The temperature in the simulations was set to 300 K and was controlled by three Nosé-Hoover thermostats, (one for each species) with a coupling frequency of  $1500 \text{ cm}^{-1}$ .<sup>60–62</sup> For the excited-state dynamics, the LR-TDDFT and ROKS methods were coupled with BO MD and Car-Parrinello MD, respectively. In both LR-TDDFT/BO MD and ROKS/Car-Parrinello MD, a time step of 5 a.u. was employed. For ROKS/Car-Parrinello MD, a fictitious mass parameter of 800 a.u. was used. Especially, for the simulation of the TAS with ROKS, 100 simulations were performed for the system that contains only the unit cell. The size of the unit cell is  $a = 8.24 \text{ \AA}$ ,  $b = 11.74 \text{ \AA}$ , and  $c = 8.20 \text{ \AA}$ , (orthorhombic phase). For the cell of 160 atoms, two simulations were performed, instead. Finally, the convolution of the spectra was done by applying Gaussian functions, employing the comp\_chem\_py package.<sup>63</sup>

## ACKNOWLEDGMENTS

U.R. gratefully acknowledges funding from the Swiss National Science Foundation via individual grant No. 200020-185092, the NCCR MUST and the Sinergia grant EPISODE. The authors thank the Swiss National Supercomputing Centre (CSCS) for the computer time.

Open Access Funding provided by Ecole Polytechnique Federale de Lausanne.

## CONFLICT OF INTEREST

The authors declare no competing financial interest.

## DATA AVAILABILITY STATEMENT

The data that support the findings of this study are openly available in Zenodo repository at <https://zenodo.org/record/5894812>.

## REFERENCES

- [1] NREL. Best research-cell efficiency chart Online; access date 18 May 2020. <http://www.nrel.gov/pv/assets/pdfs/pv-efficiencies-07-17-2018.pdf>, 1976.
- [2] A. Kojima, K. Teshima, Y. Shirai, T. Miyasaka, *J. Am. Chem. Soc.* **2009**, 131(17), 6050.
- [3] J.-H. Im, C.-R. Lee, J.-W. Lee, S.-W. Park, N.-G. Park, *Nanoscale* **2011**, 3, 4088.
- [4] H.-S. Kim, C.-R. Lee, J.-H. Im, K.-B. Lee, T. Moechl, A. Marchioro, S.-J. Moon, R. Humphry-Baker, J.-H. Yum, J. E. Moser, M. Grätzel, N.-G. Park, *Sci. Rep.* **2012**, 2, 591.
- [5] M. M. Lee, J. Teuscher, T. Miyasaka, T. N. Murakami, H. J. Snaith, *Science* **2012**, 338(6107), 643.
- [6] L. Etgar, P. Gao, Z. Xue, Q. Peng, A. K. Chandiran, B. Liu, M. K. Nazeeruddin, M. Grätzel, *J. Am. Chem. Soc.* **2012**, 134, 17396.
- [7] A. Mei, X. Li, L. Liu, Z. Ku, T. Liu, Y. Rong, M. Xu, M. Hu, J. Chen, Y. Yang, M. Grätzel, H. Han, *Science* **2014**, 345(6194), 295.
- [8] G. E. Eperon, S. D. Stranks, C. Menelaou, M. B. Johnston, L. M. Herz, H. J. Snaith, *Energy Environ. Sci.* **2014**, 7, 982.

- [9] X. Du, G. Wu, J. Cheng, H. Dang, K. Ma, Y.-W. Zhang, P.-F. Tan, S. Chen, *RSC Adv.* **2017**, *7*, 10391.
- [10] D. Yang, P. Li, Y. Zou, M. Cao, H. Hu, Q. Zhong, J. Hu, B. Sun, S. Duhm, Y. Xu, Q. Zhang, *Chem. Mater.* **2019**, *31*(5), 1575.
- [11] J. Chen, K. Židek, P. Chábera, D. Liu, P. Cheng, L. Nuuttila, M. J. Al-Marri, H. Lehtivuori, M. E. Messing, K. Han, K. Zheng, T. Pullerits, *J. Phys. Chem. Lett.* **2017**, *8*(10), 2316.
- [12] M. A. Idowu, S. H. Yau, O. Varnavski, T. Goodson, *ACS Photon.* **2017**, *4*(5), 1195.
- [13] M. Bokdam, T. Sander, A. Stroppa, S. Picozzi, D. D. Sarma, C. Franchini, G. Kresse, *Sci. Rep.* **2016**, *6*, 28618.
- [14] J. S. Manser, P. V. Kamat, *Nat. Photon.* **2014**, *8*(9), 737.
- [15] K. G. Stamplecoskie, J. S. Manser, P. V. Kamat, *Energy Environ. Sci.* **2015**, *8*(1), 208.
- [16] S. Nah, B. Spokoynny, X. Jiang, C. Stoumpos, C. M. M. Soe, M. G. Kanatzidis, E. Harel, *Nano Lett.* **2018**, *18*(2), 827.
- [17] N. Yarita, H. Tahara, T. Ihara, T. Kawawaki, R. Sato, M. Saruyama, T. Teranishi, Y. Kanemitsu, *J. Phys. Chem. Lett.* **2017**, *8*(7), 1413.
- [18] S. W. Eaton, M. Lai, N. A. Gibson, A. B. Wong, L. Dou, J. Ma, L.-W. Wang, S. R. Leone, P. Yang, *PNAS* **2016**, *113*(8), 1993.
- [19] Y. Fu, H. Zhu, C. C. Stoumpos, Q. Ding, J. Wang, M. G. Kanatzidis, X. Zhu, S. Jin, *ACS Nano* **2016**, *10*(8), 7963.
- [20] K. Park, J. W. Lee, J. D. Kim, N. S. Han, D. M. Jang, S. Jeong, J. Park, J. K. Song, *J. Phys. Chem. Lett.* **2016**, *7*(18), 3703.
- [21] Z. Liu, Q. Shang, C. Li, L. Zhao, Y. Gao, Q. Li, J. Chen, S. Zhang, X. Liu, Y. Fu, Q. Zhang, *Appl. Phys. Lett.* **2019**, *114*(10), 101902.
- [22] C. C. Stoumpos, C. D. Malliakas, J. A. Peters, Z. Liu, M. Sebastian, J. Im, T. C. Chasapis, A. C. Wibowo, D. Y. Chung, A. J. Freeman, B. W. Wessels, M. G. Kanatzidis, *Cryst. Growth Des.* **2013**, *13*(7), 2722.
- [23] K. Wu, G. Liang, Q. Shang, Y. Ren, D. Kong, T. Lian, *J. Am. Chem. Soc.* **2015**, *137*(40), 12792.
- [24] K. Wei, X. Zheng, X. Cheng, C. Shen, T. Jiang, *Adv. Opt. Mater.* **2016**, *4*(12), 1993.
- [25] J. Aneesh, A. Swarnkar, V. Kumar Ravi, R. Sharma, A. Nag, K. V. Adarsh, *J. Phys. Chem. C* **2017**, *121*(8), 4734.
- [26] A. Boziki, M. I. Dar, G. Jacopin, M. Grätzel, U. Rothlisberger, *J. Phys. Chem. Lett.* **2021**, *12*(10), 2699.
- [27] D. M. Trots, S. V. Myagkota, *J. Phys. Chem. Solids* **2008**, *69*(10), 2520.
- [28] Y. Wang, X. Li, X. Zhao, L. Xiao, H. Zeng, H. Sun, *Nano Lett.* **2016**, *16*(1), 448.
- [29] Y. Xu, Q. Chen, C. Zhang, R. Wang, H. Wu, X. Zhang, G. Xing, W. W. Yu, X. Wang, Y. Zhang, M. Xiao, *J. Am. Chem. Soc.* **2016**, *138*(11), 3761.
- [30] L. Wang, C. McCreese, A. Kovalsky, Y. Zhao, C. Burda, *J. Am. Chem. Soc.* **2014**, *136*(35), 12205.
- [31] J. Liu, J. Leng, S. Wang, J. Zhang, S. Jin, *J. Phys. Chem. Lett.* **2019**, *10*(1), 97.
- [32] A. M. A. Leguy, P. Azarhoosh, M. I. Alonso, M. Campoy-Quiles, O. J. Weber, J. Yao, D. Bryant, M. T. Weller, J. Nelson, A. Walsh, M. van Schilfhaarde, P. R. F. Barnes, *Nanoscale* **2016**, *8*(12), 6317.
- [33] J. Butkus, P. Vashishtha, K. Chen, J. K. Gallaher, S. K. K. Prasad, D. Z. Metin, G. Lauffer, N. Gaston, J. E. Halpert, J. M. Hodgkiss, *Chem. Mater.* **2017**, *29*(8), 3644.
- [34] M. C. Brennan, J. Zinna, M. Kuno, *ACS Energy Lett.* **2017**, *2*(7), 1487.
- [35] M. C. Brennan, J. E. Herr, T. S. Nguyen-Beck, J. Zinna, S. Draguta, S. Rouvimov, J. Parkhill, M. Kuno, *J. Am. Chem. Soc.* **2017**, *139*(35), 12201.
- [36] P. T. C. So, C. Y. Dong, K. M. Berland, T. French, E. Gratton, *Time-Resolved Stimulated-Emission and Transient-Absorption Microscopy and Spectroscopy*, Springer, USA **2002**, p. 427.
- [37] I. Frank, J. Hutter, D. Marx, M. Parrinello, *J. Chem. Phys.* **1998**, *108*, 4060.
- [38] S. Hirotsu, J. Harada, M. Iizumi, K. Gesi, *J. Phys. Soc. Jpn.* **1974**, *37*(5), 1393.
- [39] J. Even, L. Pedesseau, J.-M. Jancu, C. Katan, *J. Phys. Chem. Lett.* **2013**, *4*(17), 2999.
- [40] S. Meloni, G. Palermo, N. Ashari-Astani, M. Grätzel, U. Rothlisberger, *J. Mater. Chem. A* **2016**, *4*, 15997.
- [41] J. Wiktor, U. Rothlisberger, A. Pasquarello, *J. Phys. Chem. Lett.* **2017**, *8*(22), 5507.
- [42] A. Boziki, D. J. Kubicki, A. Mishra, S. Meloni, E. Lyndon, M. Grätzel, U. Rothlisberger, *Chem. Mater.* **2020**, *32*(6), 2605.
- [43] M. I. Dar, G. Jacopin, S. Meloni, A. Mattoni, N. Arora, A. Boziki, S. M. Zakeeruddin, U. Rothlisberger, M. Grätzel, *Sci Adv* **2016**, *2*(10), e1601156.
- [44] S. Collavini, S. F. Völker, J. L. Delgado, *Angew. Chem. Int. Ed.* **2015**, *54*(34), 9757.
- [45] Q. Lin, A. Armin, R. Chandra, R. Nagiri, P. L. Burn, P. Meredith, *Nat. Photon.* **2015**, *9*(2), 106.
- [46] A. Miyata, A. Mitioglu, P. Plochocka, O. Portugall, J. T.-W. Wang, S. D. Stranks, H. J. Snaith, R. J. Nicholas, *Nat. Phys.* **2015**, *11*(7), 582.
- [47] P. Hohenberg, W. Kohn, *Phys. Rev.* **1964**, *136*, B864.
- [48] W. Kohn, L. J. Sham, *Phys. Rev.* **1965**, *140*, A1133.
- [49] P. Giannozzi, S. Baroni, N. Bonini, M. Calandra, R. Car, C. Cavazzoni, D. Ceresoli, G. L. Chiarotti, M. Cococcioni, I. Dabo, A. Dal Corso, S. de Gironcoli, S. Fabris, G. Fratesi, R. Gebauer, U. Gerstmann, C. Gougoussis, A. Kokalj, M. Lazzeri, L. Martin-Samos, N. Marzari, F. Mauri, R. Mazzarello, S. Paolini, A. Pasquarello, L. Paulatto, C. Sbraccia, S. Scandolo, G. Sclauzero, A. P. Seitsonen, A. Smogunov, P. Umari, R. M. Wentzcovitch, *J. Phys. Condens. Matter* **2009**, *21*(39), 395502.
- [50] P. Giannozzi, O. Andreussi, T. Brumme, O. Bunau, M. Buongiorno Nardelli, M. Calandra, R. Car, C. Cavazzoni, D. Ceresoli, M. Cococcioni, N. Colonna, I. Carnimeo, A. Dal Corso, S. de Gironcoli, P. Delugas, R. A. DiStasio Jr., A. Ferretti, A. Floris, G. Fratesi, G. Fugallo, R. Gebauer, U. Gerstmann, F. Giustino, T. Gorni, J. Jia, M. Kawamura, H.-Y. Ko, A. Kokalj, E. Küçükbenli, M. Lazzeri, M. Marsili, N. Marzari, F. Mauri, N. L. Nguyen, H.-V. Nguyen, A. Otero-de-la Roza, L. Paulatto, S. Poncé, D. Rocca, R. Sabatini, B. Santra, M. Schlipf, A. P. Seitsonen, A. Smogunov, I. Timrov, T. Thonhauser, P. Umari, N. Vast, X. Wu, S. Baroni, *J. Phys. Condens. Matter* **2017**, *29*(46), 465901.
- [51] CPMD. Copyright IBM Corp 1990–2015, copyright MPI für Festkörperforschung Stuttgart 1997–2001. Accessed 1 July 2019. <http://www.cpmd.org/>, **1990**.
- [52] J. P. Perdew, K. Burke, Y. Wang, *Phys. Rev. B* **1996**, *54*, 16533.
- [53] L. Hedin, *Phys. Rev.* **1965**, *139*(3A), A796.
- [54] P. Umari, E. Mosconi, F. De Angelis, *Sci. Rep.* **2014**, *4*, 4467.
- [55] H. J. Monkhorst, J. D. Pack, *Phys. Rev. B* **1976**, *13*, 5188.
- [56] A. Dal Corso, *Comput. Mater. Sci.* **2014**, *95*, 337.
- [57] S. Goedecker, M. Teter, J. Hutter, *Phys. Rev. B* **1996**, *54*, 1703.
- [58] C. Hartwigsen, S. Goedecker, J. Hutter, *Phys. Rev. B* **1998**, *58*, 3641.
- [59] M. Krack, *Theor. Chem. Acc.* **2005**, *114*(1), 145.
- [60] S. Nosé, *Mol. Phys.* **1984**, *52*(2), 255.
- [61] S. Nosé, *J. Chem. Phys.* **1984**, *81*(1), 511.
- [62] W. G. Hoover, *Phys. Rev. A* **1985**, *31*, 1695.
- [63] P. Baudin. `comp_chem_py`, a python library for computational chemistry. Accessed 20 May 2020, 2019. <https://doi.org/10.5281/zenodo.2580170>.

## SUPPORTING INFORMATION

Additional supporting information may be found in the online version of the article at the publisher's website.

**How to cite this article:** A. Boziki, P. Baudin, E. Liberatore, N. Ashari Astani, U. Rothlisberger, *J. Comput. Chem.* **2022**, *43*(8), 577. <https://doi.org/10.1002/jcc.26815>